Phase II Study of Eribulin plus Pembrolizumab in Metastatic Soft-tissue Sarcomas: Clinical Outcomes and Biological Correlates

Candace L. Haddox[1], Michael J. Nathenson[1], Emanuele Mazzola[2], Jia-Ren Lin[3,4], Joanna Baginska[5], Allison Nau[2,5], Jason L. Weirather[2,5], Edwin Choy[6], Adrian Marino-Enriquez[7], Jeffrey A. Morgan[1], Gregory M. Cote[6], Priscilla Merriam[1], Andrew J. Wagner[1], Peter K. Sorger[3,4], Sandro Santagata[3,4,7], and Suzanne George[1]

ABSTRACT

Purpose: Eribulin modulates the tumor-immune microenvironment via cGAS-STING signaling in preclinical models. This non-randomized phase II trial evaluated the combination of eribulin and pembrolizumab in patients with soft-tissue sarcomas (STS).

Patients and Methods: Patients enrolled in one of three cohorts: leiomyosarcoma (LMS), liposarcomas (LPS), or other STS that may benefit from PD-1 inhibitors, including undifferentiated pleomorphic sarcoma (UPS). Eribulin was administered at 1.4 mg/m^2 i.v. (days 1 and 8) with fixed-dose pembrolizumab 200 mg i.v. (day 1) of each 21-day cycle, until progression, unacceptable toxicity, or completion of 2 years of treatment. The primary endpoint was the 12-week progression-free survival rate (PFS-12) in each cohort. Secondary endpoints included the objective response rate, median PFS, safety profile, and overall survival (OS). Pretreatment and on-treatment blood specimens were evaluated in patients who achieved durable disease control (DDC) or progression within 12 weeks [early progression (EP)]. Multiplexed immunofluorescence was performed on archival LPS samples from patients with DDC or EP.

Results: Fifty-seven patients enrolled (LMS, $n = 19$; LPS, $n = 20$; UPS/Other, $n = 18$). The PFS-12 was 36.8% (90% confidence interval: 22.5–60.4) for LMS, 69.6% (54.5–89.0) for LPS, and 52.6% (36.8–75.3) for UPS/Other cohorts. All 3 patients in the UPS/Other cohort with angiosarcoma achieved RECIST responses. Toxicity was manageable. Higher IFNα and IL4 serum levels were associated with clinical benefit. Immune aggregates expressing PD-1 and PD-L1 were observed in a patient that completed 2 years of treatment.

Conclusions: The combination of eribulin and pembrolizumab demonstrated promising activity in LPS and angiosarcoma.

Introduction

Soft-tissue sarcomas (STS) encompass a diverse group of mesenchymal malignancies with over 80 distinct subtypes. Among these subtypes, undifferentiated pleomorphic sarcoma (UPS), leiomyosarcoma (LMS), and well-differentiated/dedifferentiated liposarcoma (DDLPS) are among the most common histologies (1). The available treatment options for patients with advanced (i.e., surgically unresectable for cure) or metastatic STS are limited in number and effectiveness. Cytotoxic chemotherapy regimens are commonly used as frontline and subsequent systemic therapies in most STS subtypes. However, novel therapies and combinations are needed to expand the current repertoire of therapies to improve outcomes for patients with STS.

Eribulin exhibits potent antiproliferative effects in various cancers, an activity that is attributable to its inhibition of microtubule polymerization in tumor cells (2). Eribulin also augments the tumor microenvironment (TME) through non-mitotic mechanisms, including tumor vascular remodeling, enhanced perfusion and drug delivery, and decreased expression of immunosuppressive markers such as PD-L1 and FOXP3 (2, 3). The FDA has approved eribulin for the treatment of LPS, and eribulin has modest activity in other subtypes of STS (4, 5).

Several studies have investigated the activity of immune checkpoint inhibitors (ICI) in sarcomas. Specifically, PD-1 or PD-L1 inhibitors, either as monotherapy or in combination with the CTLA4 inhibitor ipilimumab have shown promising activity in several sarcoma subtypes, including UPS, myxofibrosarcoma (MFS), DDLPS, and angiosarcoma (6–9). Recently, the PD-L1 inhibitor atezolizumab received FDA approval for the ultra-rare STS subtype alveolar soft part sarcoma (10).

Cytotoxic chemotherapy has been reported to affect the tumor-immune microenvironment through effects on tumor-associated macrophages and neoantigen production. Recent studies have therefore investigated several immunotherapy combinations, including PD-1 or PD-L1 inhibitors combined with trabectedin, doxorubicin, and metronomic cyclophosphamide (6, 11–13). Preclinical evidence suggests that eribulin may enhance the effectiveness of immunotherapy by affecting the tumor-immune microenvironment through modulation of STING signaling (14). Eribulin was previously combined with pembrolizumab in a phase Ib/II study (ENHANCE-1) involving a heterogeneous population of patients with triple-negative breast

[1]Sarcoma Center, Department of Medical Oncology, Dana-Farber Cancer Institute, Boston, Massachusetts. [2]Department of Data Science, Dana-Farber Cancer Institute, Boston, Massachusetts. [3]Department of Systems Biology, Harvard Medical School, Boston, Massachusetts. [4]Laboratory of Systems Pharmacology, Harvard Medical School, Boston, Massachusetts. [5]Center for Immuno-Oncology, Dana-Farber Cancer Institute, Boston, Massachusetts. [6]Division of Hematology Oncology, Massachusetts General Cancer Center, Boston, Massachusetts. [7]Department of Pathology, Brigham and Women's Hospital, Boston, Massachusetts.

C.L. Haddox and M.J. Nathenson contributed equally to this article.

Current address for M.J. Nathenson: Adaptimmune LLC, Philadelphia, Pennsylvania.

Corresponding Author: Candace L. Haddox, Dana-Farber Cancer Institute, Boston, MA 02215. E-mail: Candace_haddox@dfci.harvard.edu

Clin Cancer Res 2024;30:1281–92

doi: 10.1158/1078-0432.CCR-23-2250

Translational Relevance

Although cytotoxic agents are standard-of-care therapies for metastatic or advanced/unresectable soft-tissue sarcomas (STS), these treatments are associated with only modest improvements in outcomes. One such agent is eribulin, a microtubule-binding chemotherapy approved for the treatment of liposarcomas (LPS). Preclinical evidence suggests that eribulin may enhance the efficacy of immunotherapies by modulating interferon signaling and influencing immune cell composition of the tumor microenvironment. Thus, this investigator-initiated phase II trial evaluated the safety and efficacy of combination eribulin and pembrolizumab, a PD-1 checkpoint inhibitor, in the treatment of specific STS subtypes: leiomyosarcoma, LPS, or other sarcoma subtypes in which anti-PD-1 therapy has shown benefit, including undifferentiated pleomorphic sarcoma. Correlative studies compared peripheral immune cell subsets and cytokines at day 1 and day 8 between patients with durable disease control and early progression. The combination of eribulin and pembrolizumab demonstrated promising activity in LPS and was well tolerated by patients. This study highlights the need for predictive biomarkers and a robust understanding of the immune microenvironment within histologic subtypes of STS.

cancer (TNBC). This trial demonstrated a favorable safety profile, but it did not show significant improvement in clinical outcomes (15). Given the inherent differences between TNBC and sarcomas in their respective biological underpinnings, tissue origins, and treatment paradigms, the observed improved overall survival (OS) with eribulin in STCs, and the impact of eribulin on the TME that could enhance PD-1 inhibitor activity, we hypothesized that combination eribulin and pembrolizumab may be effective in STCs. The objective of this study was to evaluate the safety and efficacy of the combination of eribulin and pembrolizumab in three histopathologically-defined cohorts of STS: LMS, LPS, and other STS known to respond to immunotherapy, including UPS. In addition, we aimed to explore the baseline immunologic characteristics of the tumors within the enrolled cohorts to identify potential predictors of response to this combination therapy.

Patients and Methods

Patients and treatment schedules

The study protocol was approved in 2019 by the Dana-Farber Cancer Institute Institutionalized Review Board (protocol available in Supplementary Materials and Methods) and was conducted in accordance with the Belmont Report, and the U.S. Common Rule. The study was registered at ClinicalTrials.gov (NCT03899805) and followed STROBE reporting guidelines. Patient enrollment took place at Dana-Farber Cancer Institute and Massachusetts General Hospital. All patients provided written informed consent. Eligible patients were required to have histologically confirmed LMS, LPS, or UPS and other sarcomas that might respond to PD-1 inhibition (UPS/Other). Initially, the UPS/Other cohort only included UPS, but an amendment was introduced to broaden eligibility criteria to include other sarcoma subtypes due to emerging reports of potential efficacy in response to immunotherapy. These "other sarcomas" included various histologies that have been reported to respond to immunotherapy such as alveolar soft part sarcoma, angiosarcoma, mismatch repair deficiency sarcomas, and other entities as determined by the principal investigator and treating physician. Key eligibility criteria included adults ages 18 years or older with advanced or metastatic measurable disease, an Eastern Cooperative Oncology Group (ECOG) performance status of 0 or 1, and having received at least one prior line of chemotherapy. Patients were ineligible if they received any prior immunotherapy including anti-PD-1, anti-PD-L1, anti-CTLA4, or OX40 agonists, and/or if they had a primary immunodeficiency or solid organ transplant. Adequate organ function was required as specified in the protocol. Upon enrollment, archival tissue was requested for confirmation of diagnosis and correlative studies.

Eribulin was administered at a dose of 1.4 mg/m^2 i.v. on days 1 and 8 of each 21-day cycle, and pembrolizumab was administered at a fixed dose of 200 mg i.v. on day 1 of each 21-day cycle. Patients continued treatment until progression, unacceptable toxicity, or for a maximum duration of 2 years (equivalent to 35 cycles). Response to treatment was assessed every 6 weeks for the first 8 cycles, according to RECIST version 1.1 (RECIST 1.1; ref. 16). Subsequently, response assessments were conducted every 12 weeks. Participants who experienced disease progression on the first response assessment but remained clinically stable were given the option to continue on treatment, with repeat response assessment after 4 weeks at the discretion of the investigator. Participants who stopped one drug due to toxicity were permitted to continue receiving the other drug as a single agent.

Trial design and endpoints

This phase II trial was designed as a parallel cohort, non-randomized, open-label trial with a primary objective of assessing the 12-week progression-free survival (PFS-12) within each cohort as determined by RECIST 1.1. Secondary objectives included assessing the objective response rate based on RECIST 1.1 and the clinical benefit rate [complete response (CR) + partial response (PR) + stable disease (SD) at 12 weeks] for the combination of eribulin and pembrolizumab in each of the three cohorts. In addition, tolerability and toxicities of the combination were assessed using the Adverse Event Severity scale based on the NCI Common Terminology Criteria for Adverse Events version 5.0. Finally, OS was measured for participants in each cohort to assess the long-term survival outcomes related to the combination treatment.

Statistical calculations

Demographic features of the participants were summarized by diagnosis subgroup using standard summary statistics such as mean, standard deviation, and range.

The primary endpoint (PFS-12) was summarized by diagnosis subgroup and analyzed for all the subgroups using Kaplan–Meier estimators with 90% confidence intervals (CI) and the survival rates across cohorts were compared using the log-rank test. PFS-12 was defined as the absence of disease progression at 12 weeks from study enrollment. For each cohort, assuming nine observed events in 19 participants, the overall power for the PFS-12 endpoint is 91% using the exact binomial distribution with 10% type I error. Within each cohort, a PFS-12 rate of 60% was considered a positive result and the null hypothesis PFS-12 rate was set to 30%. Median time to PFS and median follow-up times were calculated for each of the diagnosis subgroups. Time to progression was calculated as the difference between the enrollment date and the date of progression. Individuals who did not progress or die at any date were censored for PFS at the date of their last non-progression scan. OS (secondary endpoint) and median OS were compared using the log-rank test using 90% CIs through the completion of the study at 2 years. Toxicities were

tabulated by maximum grade and by type, in each case including the percent of high-grade toxicities (grades 3–4-5 collapsed) as well as the fraction of the total number of patients treated on study for each type. The percent change from baseline scan (sum of the longest tumor diameter on response assessments over time) was plotted across the number of weeks from registration was shown using a spider plot. In addition, the maximum decrease of this percent change in terms of sum of the longest tumor diameter for each patient was represented with a waterfall plot, again stratified by diagnosis.

Exploratory studies

Two exploratory cohorts were formed across the three main disease cohorts to investigate potential biomarkers associated with treatment outcomes. These consisted of patients who achieved durable disease control (DDC) for at least 6 months and those who experienced early RECIST-defined progression before 12 weeks [early progression (EP)].

Peripheral cytokine analysis

Plasma samples were collected from patients prior to treatment administration on cycle 1 day 1 (C1D1) and at C1D8. Samples from patients with DDC or EP across the three main cohorts were analyzed using the FLEXMAP 3D Luminex multiplex cytokine analysis platform to measure levels of the following cytokines: IL4, IL8, IL10, MCP-1, MIP-1α, MIP-1β, IL6, IL1, IL2, IFNα, TNFα, CDK4, VEGF-A TGFβ, IL2Rα, and MICB. A dilution factor of 2x was used for every cytokine. For the statistical analysis, any values below the lower limit of detection were replaced by a value of 0. The Wilcoxon rank-sum test was used to compare the levels of cytokines between the EP and DDC groups at pretreatment (C1D1) and on-treatment (C1D8) timepoints.

Cytometry by time of flight

Cytometry by time of flight (CyTOF) methods were adapted from Weber and colleagues and Nowicka and colleagues (17, 18). Peripheral blood mononuclear cells (PBMC) were isolated from C1D1 (predose) and C1D8 (on-treatment) blood samples obtained from patients with EP and DDC. The PBMC samples were cryopreserved in liquid nitrogen and thawed on the day of CyToF staining. The cells were counted using acridine orange (AO)/propidium iodide and centrifuged at 400 × *g* for 10 minutes. Cells were then incubated in viability stain for 10 minutes, washed in CyFACS and incubated with undiluted Human TruStain FcX for 10 minutes for Fc receptor blocking. A master mix of surface antibodies was added to the cell suspension and incubated for 30 minutes. The cells were then washed and fixed/permeabilized using FoxP3 Fixation/-Permeabilization Concentrate and Diluent following manufacturer's guidelines (eBioscience). Intracellular antibodies prepared with 1X Perm Wash were added to each sample and incubated for 30 minutes. The mass cytometry panel used metal-tagged antibodies; a detailed list can be found in Supplementary Table S1. The cells were washed with 1X Perm Wash and incubated overnight at 4°C in FoxP3 Fixation/Permeabilization Concentrate and Diluent, containing 191/193Ir DNA Intercalator. Mass cytometry data were collected using a CyToF XT Mass Cytometer (Standard Biotools). EQ Four Element Calibration Beads (1:10 in CAS) were used according to the manufacturer protocol before and during acquisition. The data were normalized using the FCS Processing tab of the Fluidigm CyTOF Software 7.0.8493. The detailed protocol is available (19), and Supplementary Table S1 lists the antibodies used in the panel. The CyTOF data were quantified and analyzed using the CATALYST Pipeline (17, 18).

Cyclic immunofluorescence

Cycle immunofluorescence (CyCIF) staining was performed following the methodology described in Lin and colleagues (20) on archival formalin-fixed paraffin-embedded tissue slides obtained from patients in the LPS cohort who had either EP or DDC. The unstained tissue slides underwent dewaxing and antigen retrieval processed on Leica BOND RX. Subsequently, the dewaxed slides were treated with a hydrogen peroxide solution (4.5% H_2O_2, 30 mmol/L NaOH in PBS) to reduce autofluorescent background. The slides were then stained with the antibodies and imaged with CyteFinder slide scanner (RareCyte) using a 20x objective. A detailed list of antibodies used for CyCIF can be found in Supplementary Table S2.

CyCIF image analysis

The processing and analysis of CyCIF images was conducted using the MCMICRO pipeline, which performs registration, stitching, segmentation of individual cells, and quantification of single-cell intensity data as described by Schapiro and colleagues (21). To ensure data quality, regions with obvious image artifacts (tissue folding, necrosis, antibody aggregates, etc.) were excluded during the analysis. Cells were scored for individual markers by applying Gaussian mixture modeling (for positive and negative populations) as confirmed by human inspection and inspection of intensity histograms and scatter plots. Customized MATLAB scripts were used to generate all plots (RRID: SCR_001622). The scripts and additional information can be accessed at the following GitHib repository: https://github.com/labsyspharm/DDLPS_2023.

Data availability

The trial protocol is available in the Supplementary Materials and Methods and deidentified patient-level data are available upon request from the corresponding author. The raw data for cytokine measurements and CyTOF can be provided upon request from the corresponding author. CyCIF scripts can be accessed through the following GitHib repository: https://github.com/labsyspharm/DDLPS_2023.

Results

Patient demographics

Between June 4, 2019 and February 8, 2021, eligible participants were registered in three different cohorts: LPS ($n = 20$), LMS ($n = 19$), and UPS/Other ($n = 18$). The LPS cohort included DDLPS ($n = 17$), pleomorphic LPS ($n = 2$), and myxoid LPS ($n = 1$). The UPS/Other cohort included UPS ($n = 8$), angiosarcoma ($n = 3$), spindle cell sarcoma ($n = 2$), and one of each of the following: Kaposi sarcoma, malignant peripheral nerve sheath tumor, MFS, low-grade myofibroblastic sarcoma, and SMARCA4-deficient thoracic sarcoma. Patient characteristics by cohort are summarized in **Table 1**. See Supplementary Table S3 for key STS demographics in the United States to compare with the population enrolled in this study. The average age across cohorts was 60.4 years (standard deviation 11.1, range: 29–80), and 57.9% of the participants were female. The primary site varied by cohort as expected. For example, a majority of participants in the LMS cohort had primary uterine LMS (57.9%), and a majority of participants in the LPS cohort had a primary tumor arising in the retroperitoneum (55.0%). The LMS cohort received more prior lines of systemic therapy on average (3.7, standard deviation 1.9, range: 1–7) compared with the other cohorts. The median follow-up time for OS was 104 weeks, and for PFS was 62.1 weeks for LMS, 50.4 weeks for LPS, and 30.4 weeks for the UPS/Other cohort. No patients remain on study.

Table 1. Demographics and patient characteristics by cohort.

	Leiomyosarcoma ($n = 19$)	Liposarcoma ($n = 20$)	UPS/Other ($n = 18$)	Total ($N = 57$)
Age (registration)				
Mean (standard deviation)	61.1 (8.8)	62.7 (12.6)	57.1 (11.2)	60.4 (11.1)
Range	48–80	32—78	29–73	29–80
Sex				
Female	17 (89.5%)	8 (40.0%)	8 (44.4%)	33 (57.9%)
Male	2 (10.5%)	12 (60.0%)	10 (55.6%)	24 (42.1%)
Race				
Asian	0 (0.0%)	1 (5.0%)	0 (0.0%)	1 (1.8%)
Black or African American	0 (0.0%)	0 (0.0%)	1 (5.5%)	1 (1.8%)
More than one race	1 (5.3%)	0 (0.0%)	0 (0.0%)	1 (1.8%)
Other	0 (0.0%)	1 (5.0%)	0 (0.0%)	1 (1.8%)
White	18 (94.7%)	18 (90.0%)	17 (94.4%)	53 (93.0%)
Primary site				
Extremities	0 (0.0%)	3 (15.0%)	9 (50.0%)	12 (21.1%)
Retroperitoneum	3 (15.8%)	11 (55.0%)	0 (0.0%)	14 (24.6%)
Trunk	1 (5.3%)	2 (10.0%)	2 (11.1%)	5 (8.8%)
Uterine	11 (57.9%)	0 (0.0%)	1 (5.6%)	12 (21.1%)
Other	4 (21.1%)	4 (20.0%)	6 (33.3%)	14 (24.6%)
Prior systemic therapies				
Mean (standard deviation)	3.7 (1.9)	1.7 (0.9)	1.5 (1.0)	2.3 (1.5)
Range	1.0–7.0	1.0–4.0	0.0–4.0	0.0–7.0
ECOG status				
0	10 (52.6%)	11 (55.0%)	9 (50.0%)	30 (52.6%)
1	9 (47.4%)	9 (45.0%)	9 (50.0%)	27 (47.4%)

Safety

The combination of eribulin and pembrolizumab was well-tolerated overall and observed toxicities were similar to those reported previously (15). Grade 3 or higher adverse events that were at least possibly related to the combination, as well as adverse events leading to dose modification of eribulin or discontinuation of pembrolizumab are summarized in **Table 2**. The most common treatment-related adverse events included fatigue (72%), neutropenia (56%), anemia (53%), nausea (44%), decreased appetite (42%), increased aspartate aminotransferase (AST; 33%), peripheral neuropathy (32%), and increased lipase (30%; Supplementary Table S4). The most common grade 3–5 treatment-related adverse events included neutropenia (33%), decreased white blood cell count (20%), anemia (11%), increased lipase (11%), and febrile neutropenia (9%; **Table 2**). There was one grade 5 adverse event on study: a cardiac arrest after cycle 5 of combination therapy with an attribution of "at least possibly related to treatment." The patient had a history of coronary artery disease and paroxysmal atrial fibrillation. The patient suffered a cardiac arrest at home, was revived in the field, and subsequent inpatient workup showed ventricular tachycardia without evidence of cardiac ischemia or any other etiology. The patient subsequently died because of this event.

During the study, 11 patients (19.3%) required eribulin dose modification for toxicity, and 28 patients (49.1%) required eribulin dose holds for toxicity. Seven patients (12.2%) discontinued pembrolizumab due to toxicity: 2 patients for elevated amylase (grade 3, grade 2) and lipase (grade 4, grade 3), 2 patients for grade 2 arthralgias, 1 patient for asymptomatic pancreatitis and grade 2 increased lipase, 1 patient for grade 3 pneumonitis, and 1 patient for grade 1 colitis. Four patients (7.0%) permanently stopped treatment (both eribulin and pembrolizumab) due to treatment-related toxicity: 1 patient experienced grade 4 ALT increase, 1 patient developed grade 3 elevated bilirubin and elevated AST, 1 patient developed grade 3 acute renal failure from immune-mediated nephritis, and 1 patient had grade 3 elevated lipase with radiographic findings concerning for pancreatitis. All adverse events attributed to treatment that occurred with a frequency of at least 5% at any grade are detailed in Supplementary Table S4.

Responses and outcomes

Fifty-six patients were included in the analysis of treatment response. One patient with UPS was deemed unevaluable after being hospitalized during cycle 1 and coming off study after an unplanned assessment revealed progressive disease (PD). The waterfall plot in **Fig. 1A** shows the best change in the sum of target lesion diameters from baseline imaging along with the best overall response. **Figure 1B** shows the spider plot for individual patient data across the cohorts. Supplementary Figure S1 shows additional spider plots for each LPS histology (Supplementary Fig. S1A) and for UPS/Other histologies (Supplementary Fig. S1B). **Table 3** provides a summary of the 12-week PFS rate, best response, and clinical benefit rate in each cohort.

In the LMS cohort ($n = 19$), the best overall response included 2 (10.5%) with PR, 8 (42.1%) with SD, and 9 (47.4%) with PD. In the LPS cohort ($n = 20$), the best overall response included 3 (15.0%) with PR, 12 (60.0%) with SD, and 5 (25.0%) with PD. One patient with DDLPS completed all 35 cycles as per protocol and achieved a best response of SD. The LPS cohort included 17 patients with DDLPS (2 PR, 11 SD, 4 PD), 2 patients with pleomorphic LPS (1 PR, 1 PD) and 1 patient with myxoid LPS (SD). In the UPS/Other cohort ($n = 18$), best overall responses included 1 (5.6%) CR, 5 (27.8%) PR, 2 (11.1%) with SD, 9 (50%) with PD, and 1 unevaluable (5.6%). The patient on study who achieved CR had radiotherapy-associated angiosarcoma and completed 35 cycles of treatment (eribulin alone after cycle 8, pembrolizumab discontinued at cycle 8 for grade 2 lipase elevation and grade 2

Table 2. Treatment-related adverse events ≥ grade 3.

Adverse event term	Grade ≥3, *n* (%)	Any grade, *n* (%)	Pembrolizumab discontinuation	Eribulin dose modification
Neutrophil count decreased	18 (33%)	32 (56%)		Y
White blood cell decreased	11 (20%)	31 (54%)		
Anemia	6 (11%)	30 (53%)		Y
Lipase increased	5 (9%)	17 (30%)	Y	
Febrile neutropenia	5 (9%)	6 (11%)		Y
Fatigue	3 (6%)	41 (72%)		Y
Aspartate aminotransferase increased	3 (6%)	19 (33%)		
Peripheral sensory neuropathy	2 (4%)	18 (32%)		Y
Alanine aminotransferase increased	2 (4%)	13 (23%)		
Diarrhea	2 (4%)	12 (21%)		
Dyspnea	2 (4%)	10 (18%)		
Weight loss	1 (2%)	17 (30%)		Y
Hyponatremia	1 (2%)	15 (26%)		
Mucositis oral	1 (2%)	11 (19%)		Y
Serum amylase increased	1 (2%)	11 (19%)	Y	
Arthralgia	1 (2%)	9 (16%)	Y	
Blood bilirubin increased	1 (2%)	4 (7%)		
Pain in extremity	1 (2%)	3 (5%)		
Lymphocyte count decreased	1 (2%)	2 (4%)		
Pancreatitis	1 (2%)	2 (4%)	Y	
Pneumonitis	1 (2%)	2 (4%)	Y	
Acute kidney injury	1 (2%)	1 (2%)		Y
Cardiac arrest*	1 (2%)*	1 (2%)*		
Hepatitis viral	1 (2%)	1 (2%)		
Lymphocyte count increased	1 (2%)	1 (2%)		
Constipation	0 (0%)	15 (26%)		Y
Colitis	0 (0%)	3 (5%)	Y	

Note: Adverse events at least possibly related to the treatment regimen (grade 3 or higher, or leading to dose modification) are included. $N = 57$; asterisk (*) denotes grade 5 event. Events leading to discontinuation of pembrolizumab and events leading to dose modification of eribulin are noted in the second column from right, and in the final column, respectively, with "Y".

arthralgia, requiring treatment with methotrexate). Notably, all 3 patients with angiosarcoma (cutaneous, splenic, and radiotherapy-associated breast) responded to treatment as defined by RECIST. The 3 additional patients in the UPS/Other cohort who responded had PR, and included UPS ($n = 2$) and SMARCA4-deficient thoracic sarcoma ($n = 1$).

Only the LPS cohort met the primary endpoint of 12-week PFS rate >60% (**Table 3**). The 12-week PFS rate (with 90% lower/upper CI) was 36.8% (22.5–60.4) for LMS, 69.6% (54.5–89.0) for LPS, and 52.6% (36.8–75.3) for UPS/Other cohorts. The median PFS was 11.1 weeks (6.5–18.7) for LMS, 31.7 weeks [12.4–not reached (NR)] for LPS, and 12.4 weeks (6.1–30.4) for the UPS/Other cohorts (**Fig. 1C**). OS at 1 year was 55.6% (90% CI: 39.3–78.6) for LMS, 75.0% (90% CI: 60.7–92.7) for LPS, and 52.6% (90% CI: 36.8–75.3) for UPS/Other cohorts. Median OS was 59.1 weeks (38.1–NR) for LMS, 97.6 weeks (65.4–NR) for LPS, and NR (39.9–NR) for the UPS/Other cohorts (**Fig. 1D**).

Correlative analyses

To investigate the factors associated with DDC lasting more than 6 months and early progression within 12 weeks, we formed two exploratory cohorts. An "early progression" (EP) cohort consisted of participants with RECIST progression within 12 weeks of initiating treatment ($n = 19$), and a "durable disease control" (DDC) cohort consisting of participants with SD or PR that lasted longer than 6 months ($n = 12$). Molecular profiling was available for 11 participants (35.4%). Among these, 7 participants were from the EP cohort and 4 participants were from the DDC cohort. One patient in the DDC cohort had a SMARCA4-deficient thoracic sarcoma with high tumor mutation burden (TMB) of 10.6 mutations/Mb. All other patients with available TMB in both cohorts had low TMB.

Across the three arms, 17 patients with EP and 12 patients with DDC had paired blood specimens collected at two timepoints: pre-treatment (C1D1) and on-treatment (C1D8). Among the cytokines analyzed, IFNα and IL4 levels were significantly higher in patients with DDC compared with patients with EP at both timepoints (**Fig. 2A**). Results of other cytokines tested are included in Supplementary Fig. S2, and none of them showed a significant difference between patients with DDC and EP. PBMCs were also analyzed in patients from the LPS cohort with DDC ($n = 7$) or EP ($n = 3$) at C1D1 and C1D8 with the cell type abundance proportions displayed in **Fig. 2B**. The EP LPS cohort had a significantly higher abundance of $CD57^+$ $CD4^+$ effector memory (EM) cells at both timepoints compared with the DDC LPS cohort, but otherwise there were no significant differences between immune subset proportions in DDC LPS and EP LPS cohorts (**Fig. 2C**). IFNγ expression and granzyme B expression were higher post treatment in patients with LPS with EP across several immune subsets (**Fig. 2D**). IFNγ was higher after treatment in patients with EP in late memory $CD8^+$ T cells (EM, terminally differentiated EM, and senescent terminally differentiated EM), and non-classical monocytes (adjusted P value < 0.1). Granzyme B was significantly higher after treatment in patients with EP in late memory $CD8^+$ T cells (EM and senescent terminally differentiated EM), regulatory T cells, B cells, myeloid-derived suppressor cells,

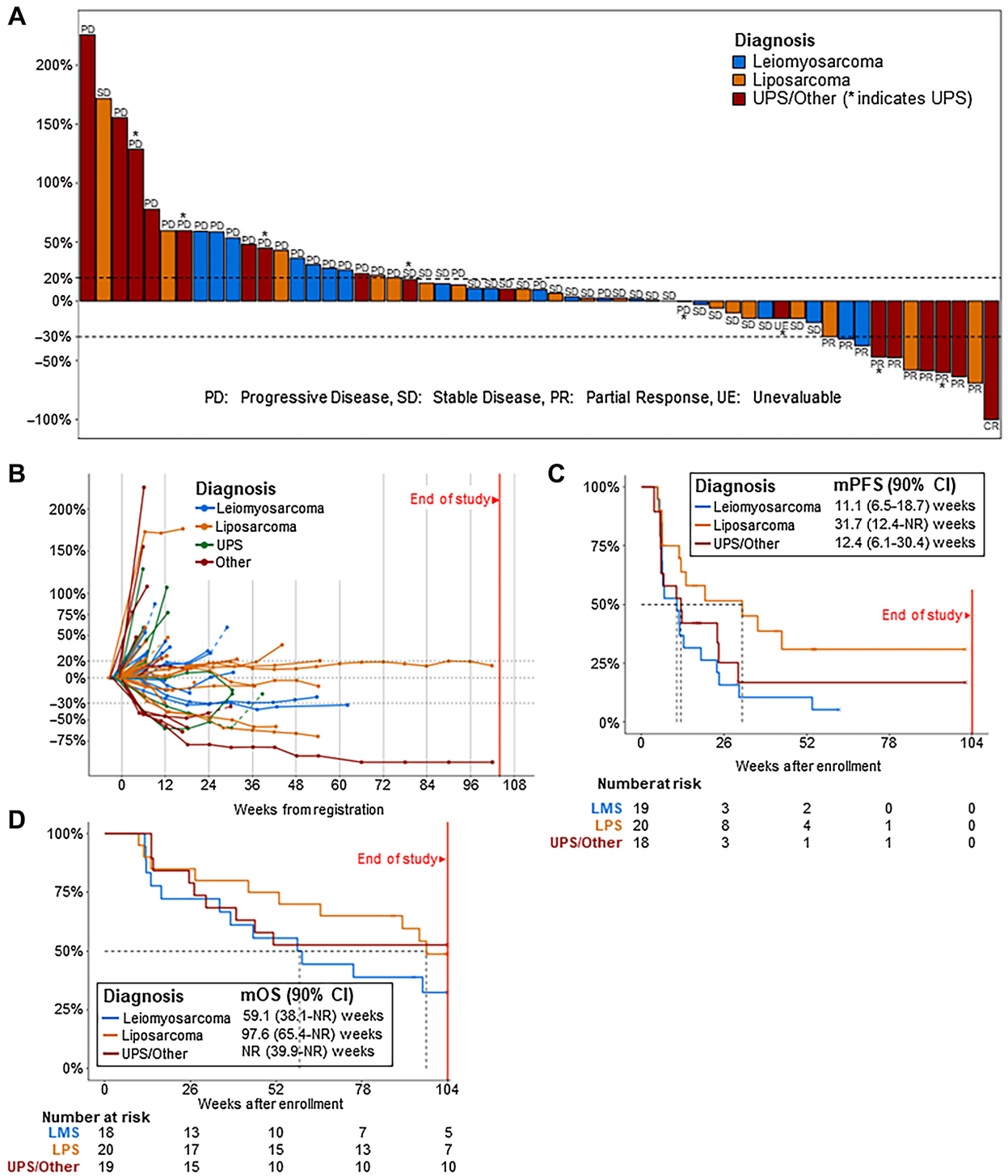

Figure 1.

Tumor response and survival. Best change from baseline scan (sum of longest tumor diameters, %) shown in waterfall plot (**A**). Duration on treatment shown in spider plot showing the change in sum of longest tumor diameters (%) compared with baseline scan across response assessments (**B**). The continuous lines in the spider plot represent the percent change in most relevant tumor measurement before progression (if any). The dashed lines represent the percent change in the most relevant tumor measurement after progression (if any). Kaplan–Meier curves of PFS (**C**) and OS (**D**). Asterisks (*) indicate UPS. CI, confidence interval; LMS, leiomyosarcoma; LPS, liposarcoma; mOS, median overall survival; mPFS, median progression free survival; PD, progressive disease; PR, partial response; SD, stable disease; UE, unevaluable; UPS, undifferentiated pleomorphic sarcoma.

Table 3. PFS rate and best response per RECIST 1.1 by cohort.

	Leiomyosarcoma ($n = 19$)	Liposarcoma ($n = 20$)	UPS/Other ($n = 18$)	Total ($N = 57$)
12-week PFS rate, % (90% CI)	36.8 (22.5–60.4)	69.6 (54.5–89.0)	52.6 (36.8–75.3)	
Best response, *N* (%)				
Progressive disease	9 (47.4%)	5 (25.0%)	9 (50.0%)	23 (40.4%)
Stable disease	8 (42.1%)	12 (60.0%)	2 (11.1%)	22 (38.6%)
Partial response	2 (10.5)	3 (15.0)	5 (27.8%)	10 (17.5%)
Complete response	0	0	1 (5.6%)	1 (1.8%)
Unevaluable	0	0	1 (5.6%)	1 (1.8%)
Clinical benefit rate, *N* (%)	10 (52.6%)	15 (75.0%)	8 (44.4%)	33 (57.9%)

Note: Clinical benefit calculated as stable disease + partial response + complete response.
Abbreviations: CI, confidence interval; PFS, progression-free survival; UPS, undifferentiated pleomorphic sarcoma.

monocytes (classical and non-classical) and dendritic cells (adjusted *P* value < 0.1; **Fig. 2D**).

Available archival tissues were analyzed in a subset of patients with LPS with DDC ($n = 7$) and EP ($n = 2$). We performed multiplexed tissue imaging using CyCIF, quantifying single cell intensities for each of the markers and using these data to define immune cell subsets. Because of the small sample sizes, statistical analysis was not performed. Expression of immune subset markers, functional markers, and checkpoints for each individual patient is shown in the heat map in **Fig. 3A**. The percentage of cells with PD-1 and PD-L1 expression are shown in **Fig. 3B**. The interaction between PD-L1– and PD-1–expressing cells was found to be more prominent in a patient with extended DDC (DDC6; **Fig. 3C**) and less prominent in an early progressor (EP2; **Fig. 3C**). In the same DDC sample (DDC6), PD-L1+ cells, $CD8^+$ cells, and $CD20^+$ cells were enriched in regions with PD-1+ cells (**Fig. 3D** and **E**). Finally, we observed immune cell aggregates in the DDC6 sample, with PD-L1–expressing macrophages in proximity with PD-1–expressing cells (**Fig. 3F**).

Discussion

Overall, the combination of eribulin and pembrolizumab was well tolerated and showed clinically meaningful activity, particularly in the LPS and UPS/Other cohorts.

The observed toxicity profile for the combination in our study was similar to previous observations as have been reported in patients with TNBC on the ENHANCE-1 trial (15); however, we did observe a numerically higher rate of high-grade neutropenia (32% vs. 26%), leukopenia (19% vs. 5.4%), and any grade anemia (53% vs. 28.1%). The rate of peripheral neuropathy was lower in our study (41.3% vs. 32%), possibly reflecting differences in study populations with respect to the number and intensity of prior therapy lines (15). In our study, there was one grade 5 event (cardiac arrest) which was possibly attributed to the combination. A single fatal case of cardiac arrest was also observed on the ENHANCE-1 trial, but was not directly attributed to the treatment.

Eribulin monotherapy has been approved by the FDA for the treatment of LPS based on an OS benefit demonstrated in the phase III trial that included 143 patients with dedifferentiated, myxoid, or pleomorphic LPS who had received at least two prior lines of therapy (5). In that trial, the 12-week progression-free rate in the LPS cohort was 40.8%, and the median PFS was 2.9 months. Similar outcomes were observed in the phase II single-arm study (SARC028), which investigated pembrolizumab monotherapy in patients with LMS, LPS, UPS, and synovial sarcoma (7, 8). The final analysis of the LPS expansion cohort revealed a 12-week progression-free rate of 44% and a median PFS of 2.0 months (8). While cross-trial comparisons should be interpreted with caution, it is notable that in our study, the combination of eribulin and pembrolizumab demonstrated promising activity in LPS, with a 12-week progression-free rate of 70.0% (90% CI: 55.0–89.1) and a median PFS of 7.4 months, possibly suggesting meaningful activity of this combination in the treatment of LPS. Further evaluation of the combination in a randomized trial with a monotherapy comparator arm in patients with LPS is needed to definitively determine whether the combination is superior to either single agent.

The UPS/Other cohort of our study demonstrated similar outcomes observed in other studies investigating PD-1 inhibitors in similar patient populations. In the SARC028 trial, pembrolizumab monotherapy demonstrated modest activity in UPS with a 12-week progression-free rate of 50% and median PFS of 3 months (95% CI: 2–5 months; ref. 8). These results are consistent with the findings in our study, which showed a 12-week PFS rate of 62.5% and median PFS of 12.6 weeks in the 8 patients with UPS included in our study. We observed PRs in all 3 patients with angiosarcoma (2 PR, 1 CR), 1 patient with SMARCA4-deficient thoracic sarcoma, and 2 out of 8 patients with UPS, which align with other reports suggesting checkpoint inhibitor activity in these specific sarcoma subtypes (22, 23). Of note, an ongoing phase II study is investigating the use of eribulin monotherapy in angiosarcoma and epithelioid hemangioendothelioma which will provide further insights into the activity of eribulin in vascular sarcomas (NCT03331250). Overall, the responses observed in the UPS/Other cohort in our study may have been primarily driven by pembrolizumab rather than the combination with eribulin, although this cannot be confirmed in the absence of a comparator arm.

The combination of eribulin and pembrolizumab showed disappointing activity in the LMS cohort with a 12-week progression-free rate of 36.8%. This response rate is similar to eribulin monotherapy observed in other studies (24, 25). Although some retrospective reports have indicated higher response rates to immunotherapy in LMS (26), our study aligns with other findings that suggest limited activity of PD-1 inhibitors in this disease, even when combined with eribulin.

Our study emphasizes the need for predictive biomarkers and a comprehensive understanding of the tumor-immune microenvironment within different histologic subtypes of sarcomas. Biomarkers that have shown predictive value in other types of cancer have proven to be unreliable for predicting response to checkpoint inhibitors in sarcomas. For example, an analysis of samples from SARC028 revealed that only 5% of tumors were PD-L1+, and responses to treatment were

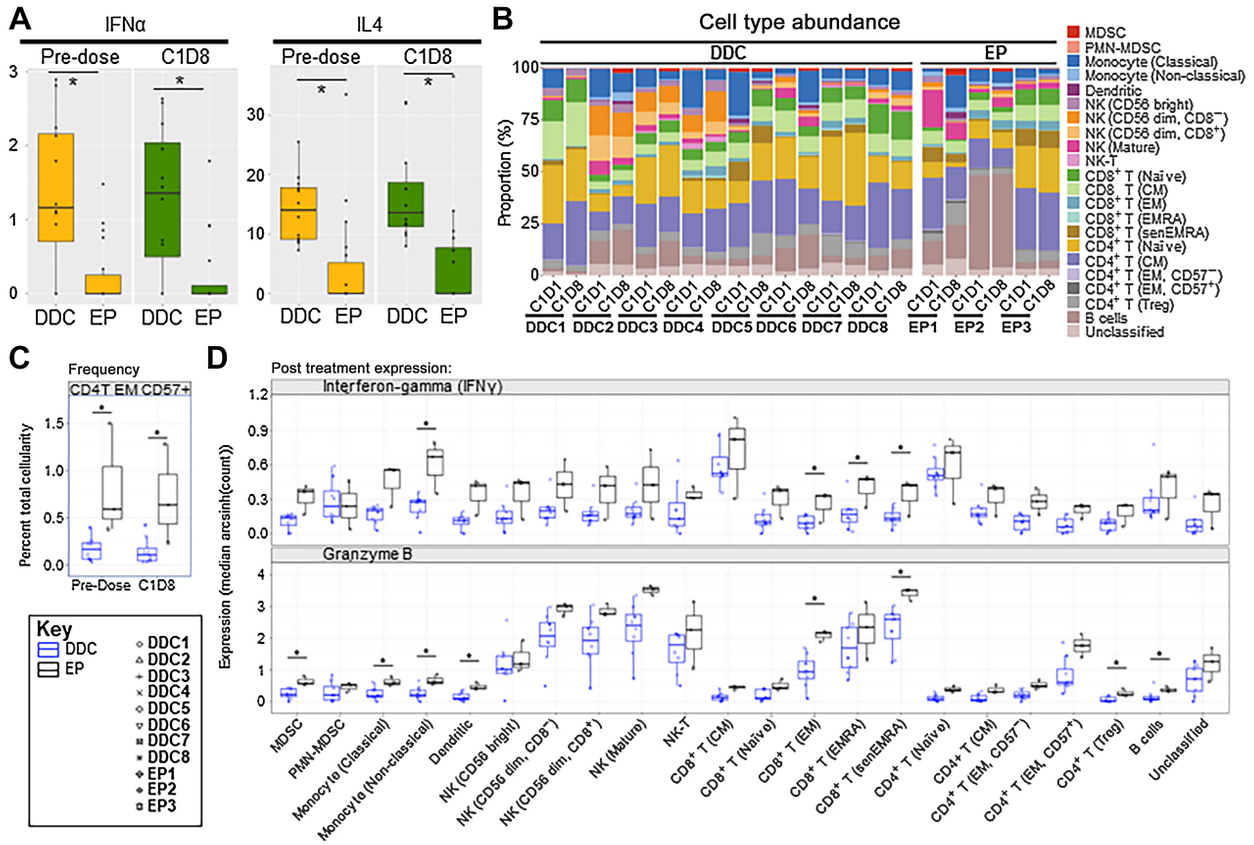

Figure 2.

Serum cytokines and PBMC subsets in patients with DDC or EP. **A,** IFNα and IL4 serum levels in patients with DDC or EP at predose and C1D8. Wilcoxon rank-sum test $P < 0.05$. **B,** PBMC cell type abundance across individual cases from the liposarcoma cohort with DDC or EP. **C,** Peripheral $CD4^+$ EM $CD57^+$ cell abundance in patients with liposarcoma with DDC versus EP at predose and C1D8, adjusted P value of 0.035 and 0.099. **D,** C1D8 expression of IFNγ (top) and granzyme B (bottom) across immune subsets in cases from the liposarcoma cohort with DDC or EP, adjusted P value < 0.1 where shown. Key for **C** and **D** shown in lower left box. CM, central memory; EM, effector memory; MDSC, myeloid-derived suppressor cells; NK, natural killer; PMN, polymorphonuclear neutrophils; RA, CD45RA+; sen, senescent; Treg, regulatory T cells.

observed in the absence of PD-L1 expression (27). In patients with angiosarcoma, high TMB has been associated with responders, but there have also been responses observed in tumors with low TMB (28). In our study, all but one of the patients with available TMB data had low TMB, including 3 of 4 patients with DDC and the patient with angiosarcoma that achieved a CR.

In an effort to identify potential predictive biomarkers of treatment response, we analyzed specimens from patients who experienced DDC and EP. Our analysis revealed higher levels of IFNα and IL4 in patients with DDC. IL4 is a cytokine associated with T helper 2 (TH2) cells that plays a role in various immune responses such as B-cell immunoglobulin class switching to IgE, proliferation of allergic reaction effectors like eosinophils and mast cells, and macrophage polarization to M2-like phenotypes (29). In carcinomas, IL4 promotes M2-like macrophage polarization (30). Interestingly, macrophages expressing PD-L1 are frequently observed in the sarcoma microenvironment and have been associated with response to immunotherapy (27, 31). Further work is needed to explore the potential link between IL4, macrophage polarization, and response to PD-1 inhibition.

Eribulin increases type 1 IFNs through activation of the cGAS-STING pathway (14). Although we found elevated levels of the type 1 IFNα in patients with DDC, we did not observe a change in circulating IFNα levels between baseline and C1D8. As such, our data did not reveal a treatment effect on circulating biomarkers from the STING/cGas pathway. Rather, IFNα levels were elevated at both timepoints in patients with DDC compared with those with EP. In the TME, IFNα can enhance antigen presentation, suppress regulatory T cells, and increase the production of cytokines that mediate immune cell cross-talk, which may prime the antitumor immune response (32). IFNα is also known to have antitumoral effects and has been studied in clinical trials in sarcomas (33, 34). However, the role of circulating IFNα in predicting response to immunotherapy is not clear. Notably, the ENHANCE-1 clinical trial evaluating the combination of eribulin and pembrolizumab in patients with TNBC did not find a difference in IFNα levels between patients who had no response versus those that received clinical benefit (35), although this may be related in part to the disease context. Future work could explore whether IFNα levels have predictive biomarker potential in patients with liposarcoma receiving immunotherapy.

Emerging evidence suggests tertiary lymphoid structures (TLS) may serve as a potential indicator of immunotherapy response (13, 36, 37). Mature TLS are characterized by the presence of a germinal center B-cell zone containing follicular dendritic cells with T cells localized to the periphery (38). A phase II study (PEMBROSARC) evaluated the combination of pembrolizumab and metronomic low-dose cyclophosphamide in an unselected population of sarcomas and was later

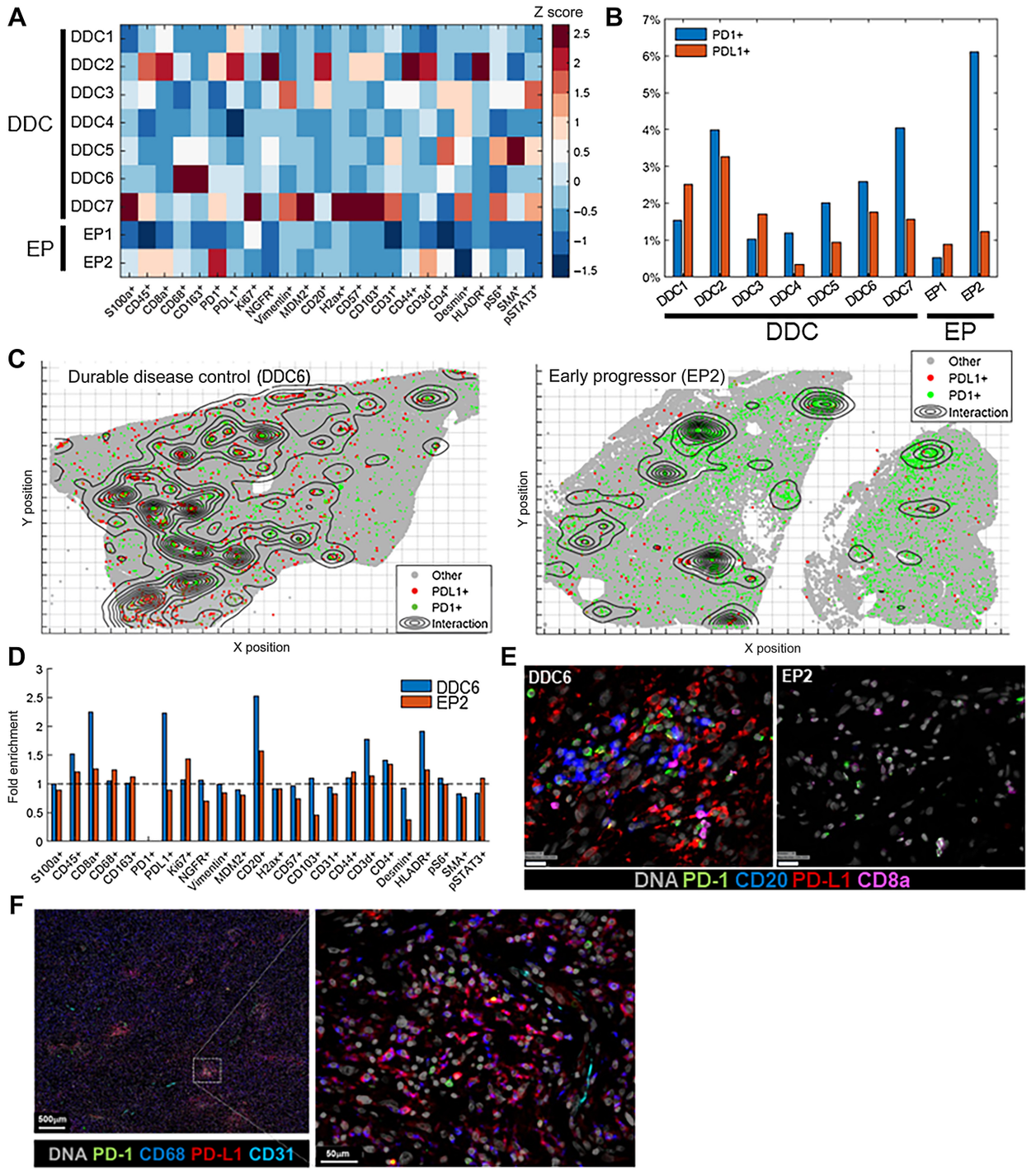

Figure 3.

Immune subsets and checkpoint expression in liposarcoma cases with DDC or EP. **A,** Heat map of CyCIF data from DDLPS samples with DDC or EP. Colors represent the Z scores of indicated cell counts, and dendrograms were generated by complete lineages using Euclidean distance matrix. **B,** PD-1+ and PD-L1+ cell counts in DDC and EP DDLPS samples. **C,** PD-1–PD-L1 interaction maps from case DDC6 and case EP2. The Spatial plots represent PD-1+ cells (green), PD-L1+ cells (red) and their interactions (black contour lines). The interaction was calculated by any given PD-1+ and PD-L1+ pairs within 20 um radius. The quantification is calculated by total number of PD-1–PD-L1 pairs divided by PD-1+ cells. **D,** PD-1+ neighborhood enrichment analysis. Bars represent the counts of each marker from cells within a 20um radius of any given PD-1+ cells, normalized by the total counts of each marker. The dotted line (ratio equal to 1) indicates no enrichment. **E,** Representative CyCIF images of PD-1+ neighborhoods from the case DDC6 and case EP2. Scale bar = 20 μm. **F,** Representative CyCIF image of immune checkpoint–expressing cell aggregates from case DDC6.

amended to restrict enrollment to TLS+ STSs (13). All patients achieving PR in that study had TLS observed in their tumor samples, suggesting that TLS may be associated with response to PD-1 inhibition (13). We therefore asked whether highly multiplexed imaging methods such as CyCIF could identify immune characteristics associated with clinical benefit in our study. We performed an analysis of archival tissue from a subset of patients with LPS and identified immune aggregates in the patient with DDC for 2 years. These aggregates appeared to have a distinct architecture with CD68 and PD-L1–expressing macrophages mixed with B cells and $CD8^+$ T cells. While these immune networks do not represent conventional TLS, they may be related to the lymphonets we have recently described in other tumor types (39), which are proposed to reflect functional interactions among different immune cell types. It is also noteworthy that the primary source of PD-L1 in proximity to $CD8^+$ cells appears to be myeloid and not tumor cells; this is consistent with CyCIF data from other solid tumors (40). These findings demonstrate the feasibility of high-plex imaging of the STS TME and argue for the future study of immune aggregates and their association with response to the eribulin/pembrolizumab combination.

The limitations of this study include limited sample size, significant heterogeneity within the UPS/Other cohort, and few archival tissue specimens. While these factors may limit interpretation and generalizability of these data, the information garnered from this small signal-seeking study supports further evaluation of combined pembrolizumab and eribulin for liposarcomas. We acknowledge that the trial design and use of combination therapy without a comparator arm precludes a formal assessment of potential synergy or additivity with eribulin and pembrolizumab. While the rationale for ICI combinations is often rooted in potential for drug synergy (as in this study), the improved outcomes observed in trials investigating ICI combinations are likely due to an individual drug in the combination (41, 42). A recent analysis of 13 phase III clinical trials evaluating potentially synergistic ICI combination therapies suggested that the improved outcomes were consistent with a model of independent drug action; in other words, the clinical benefit was explainable by the monotherapy activity and combination regimens merely increase the odds of response. Thus, in our study, it is possible that the observed responses were due to the activity of one drug rather than a synergistic combination (43) or that using pembrolizumab and eribulin in sequence rather than in combination would have similar outcomes.

In addition, the correlative analyses involving histologic samples in this study are limited by availability of archival tissues and the absence of required on-study biopsies to assess for changes in the tumor-immune microenvironment. In particular, detecting treatment-related changes in cGAS-STING pathway activation in the TME may have been informative in context with the circulating cytokine analysis performed on blood specimens.

In summary, the combination of pembrolizumab and eribulin was well tolerated and demonstrated promising activity in patients with liposarcomas, which warrants further investigation and exploration of predictive biomarkers. A larger, randomized study is needed to definitively establish the activity of this regimen in patients with liposarcoma and improve upon the currently limited repertoire of therapies. The responses observed in patients with UPS and other sarcomas are consistent with the outcomes of immunotherapy monotherapy reported in previous studies. Most notably, all 3 patients with angiosarcoma achieved an objective response defined by RECIST, including one durable CR, which may also reflect sensitivity to microtubule inhibition. In the case of LMS, the activity was similar to the limited efficacy of eribulin and PD-1 inhibitor monotherapies, suggesting additional investigations on the LMS tumor-immune microenvironment are needed to develop novel immunotherapy strategies in this disease.

Authors' Disclosures

C.L. Haddox reports other support from Merck, McEvoy Ball Family Fund, Catherine England Leiomyosarcoma Fund, and David Liposarcoma Research Initiative, as well as non-financial support from Merck and Eisai during the conduct of the study; C.L. Haddox also reports other support from HiFiBio Therapeutics, Tango Therapeutics, Aadi Biosciences, Merck KGaA/EMD-Serono, and Roche, as well as personal fees from HMP Global outside the submitted work. M.J. Nathenson reports other support from Adaptimmune outside the submitted work. E. Mazzola reports personal fees from The VeraMedica LLC outside the submitted work. E. Choy reports other support from Novartis, Merck, Tracon, and Eli Lilly, as well as personal fees from Bayer, Epizyme, and Adaptimmune outside the submitted work. A. Marino-Enriquez reports grants from NCI of the NIH (SPORE P50CA272170), The Behar's LMSARC (from the Sarcoma Alliance for Research Through Collaboration, SARC), and LMS:360 program outside the submitted work. G.M. Cote reports grants from Eisai during the conduct of the study. G.M. Cote also reports other support from BioAtla and Gilead; personal fees from Sonata; grants and personal fees from Eisai, Foghorn Therapeutics, Ikena, and C4 Therapeutics; and grants from Daiichi, Servier, PharmaMar, MacroGenics, Merck/EMD-Serono, SpringWorks, Repare Therapeutics, Kronos, Bavarian Nordic, and Pyxis outside the submitted work. P. Merriam reports other support from DFCI and U2C-CA233262, as well as grants from Merck and Eisai during the conduct of the study; P. Merriam also reports other support from Mereo Biopharma and Springworks outside the submitted work. A.J. Wagner reports grants and personal fees from Aadi Bioscience, Boehringer-Ingelheim, Cogent Biosciences, Daiichi-Sankyo, Deciphera, and Eli Lilly; personal fees from InhibRx, Kymera, PharmaEssentia, and Servier; and grants from Foghorn Therapeutics and Rain Therapeutics outside the submitted work. P.K. Sorger reports personal fees from RareCyte Inc, Applied Biomath LLC, Montai Health, NanoString, and Merck, as well as other support from Glencoe Inc during the conduct of the study. S. George reports non-financial support from Merck, as well as grants and non-financial support from Eisai during the conduct of the study. S. George also reports personal fees and other support from Blueprint Medicines, Deciphera, and BioAtla; other support from Daiichi Sankyo, Tracon, Springworks, IDRX, NewBay, and Theseus; and personal fees from Kayothera and Immunicum outside the submitted work. No disclosures were reported by the other authors.

Authors' Contributions

C.L. Haddox: Conceptualization, formal analysis, investigation, writing–original draft, writing–review and editing. **M.J. Nathenson:** Conceptualization, funding acquisition, investigation, writing–review and editing. **E. Mazzola:** Data curation, formal analysis, methodology, writing–review and editing. **J.-R. Lin:** Formal analysis, investigation, methodology, writing–review and editing. **J. Baginska:** Formal analysis, investigation, methodology, writing–review and editing. **A. Nau:** Formal analysis, methodology, writing–review and editing. **J.L. Weirather:** Formal analysis, methodology, writing–review and editing. **E. Choy:** Investigation, writing–review and editing. **A. Marino-Enriquez:** Investigation, writing–review and editing. **J.A. Morgan:** Investigation, writing–review and editing. **G.M. Cote:** Investigation, writing–review and editing. **P. Merriam:** Investigation, writing–review and editing. **A.J. Wagner:** Investigation, writing–review and editing. **P.K. Sorger:** Formal analysis, supervision, funding acquisition, writing–review and editing. **S. Santagata:** Formal analysis, supervision, investigation, writing–review and editing. **S. George:** Conceptualization, supervision, funding acquisition, investigation, methodology, writing–review and editing.

Acknowledgments

We first thank the patients, caregivers, and families who generously contributed to this study. This study was supported by Merck, which provided pembrolizumab, and Eisai, which provided eribulin and funding for this study. This study was partly funded by philanthropic support from the McEvoy Ball Family

Fund, the Catherine England Leiomyosarcoma Fund, the Ludwig Center at Harvard Medical School, the David Liposarcoma Research Initiative, and by a NIH/NCI grant (U2C-CA233262). We thank Dr. George Demetri for meaningful discussions on the design and results of this study, and Dr. Jason Hornick for pathology consultation. We acknowledge Susan Pierce, PhD, who provided medical writing assistance, and Haley E. Szewczuga who provided proofreading and submission support.

Note

Supplementary data for this article are available at Clinical Cancer Research Online (http://clincancerres.aacrjournals.org/).

Received August 2, 2023; revised October 19, 2023; accepted January 12, 2024; published first January 18, 2024.

References

1. World Health Organization (WHO) classification of tumours editorial board. Soft tissue and bone tumours. WHO classification of tumours series. 5th ed. Lyon, France: International Agency for Research on Cancer; 2020. vol. 3.
2. Cortes J, Schöffski P, Littlefield BA. Multiple modes of action of eribulin mesylate: emerging data and clinical implications. Cancer Treat Rev 2018;70: 190–8.
3. Goto W, Kashiwagi S, Asano Y, Takada K, Morisaki T, Fujita H, et al. Eribulin promotes antitumor immune responses in patients with locally advanced or metastatic breast cancer. Anticancer Res 2018;38:2929–38.
4. Schöffski P, Chawla S, Maki RG, Italiano A, Gelderblom H, Choy E, et al. Eribulin versus dacarbazine in previously treated patients with advanced liposarcoma or leiomyosarcoma: a randomised, open-label, multicentre, phase 3 trial. Lancet 2016;387:1629–37.
5. Demetri GD, Schöffski P, Grignani G, Blay JY, Maki RG, Van Tine BA, et al. Activity of eribulin in patients with advanced liposarcoma demonstrated in a subgroup analysis from a randomized phase III study of eribulin versus dacarbazine. J Clin Oncol 2017;35:3433–9.
6. Roulleaux Dugage M, Nassif EF, Italiano A, Bahleda R. Improving immunotherapy efficacy in soft-tissue sarcomas: a biomarker driven and histotype tailored review. Front Immunol 2021;12:775761.
7. Tawbi HA, Burgess M, Bolejack V, Van Tine BA, Schuetze SM, Hu J, et al. Pembrolizumab in advanced soft-tissue sarcoma and bone sarcoma (SARC028): a multicentre, two-cohort, single-arm, open-label, phase 2 trial. Lancet Oncol 2017;18:1493–501.
8. Burgess MA, Bolejack V, Schuetze SM, Tine BAV, Attia S, Riedel RF, et al. Clinical activity of pembrolizumab (P) in undifferentiated pleomorphic sarcoma (UPS) and dedifferentiated/pleomorphic liposarcoma (LPS): final results of SARC028 expansion cohorts. J Clin Oncol 37:15s, 2019 (suppl; abstr 11015).
9. D'Angelo SP, Mahoney MR, Van Tine BA, Atkins J, Milhem MM, Jahagirdar BN, et al. Nivolumab with or without ipilimumab treatment for metastatic sarcoma (Alliance A091401): two open-label, non-comparative, randomised, phase 2 trials. Lancet Oncol 2018;19:416–26.
10. Chen AP, Sharon E, O'Sullivan-Coyne G, Moore N, Foster JC, Hu JS, et al. Atezolizumab for advanced alveolar soft part sarcoma. N Engl J Med 2023;389: 911–21.
11. Wagner MJ, Zhang Y, Cranmer LD, Loggers ET, Black G, McDonnell S, et al. A phase 1/2 trial combining avelumab and trabectedin for advanced liposarcoma and leiomyosarcoma. Clin Cancer Res 2022;28:2306–12.
12. Toulmonde M, Brahmi M, Giraud A, Chakiba C, Bessede A, Kind M, et al. Trabectedin plus durvalumab in patients with advanced pretreated soft tissue sarcoma and ovarian carcinoma (TRAMUNE): an open-label, multicenter phase Ib study. Clin Cancer Res 2022;28:1765–72.
13. Italiano A, Bessede A, Pulido M, Bompas E, Piperno-Neumann S, Chevreau C, et al. Pembrolizumab in soft-tissue sarcomas with tertiary lymphoid structures: a phase 2 PEMBROSARC trial cohort. Nat Med 2022;28: 1199–206.
14. Fermaintt CS, Takahashi-Ruiz L, Liang H, Mooberry SL, Risinger AL. Eribulin activates the cGAS-STING pathway via the cytoplasmic accumulation of mitochondrial DNA. Mol Pharmacol 2021;100:309–18.
15. Tolaney SM, Kalinsky K, Kaklamani VG, D'Adamo DR, Aktan G, Tsai ML, et al. Eribulin plus pembrolizumab in patients with metastatic triple-negative breast cancer (ENHANCE 1): a phase Ib/II study. Clin Cancer Res 2021;27: 3061–8.
16. Eisenhauer EA, Therasse P, Bogaerts J, Schwartz LH, Sargent D, Ford R, et al. New response evaluation criteria in solid tumours: revised RECIST guideline (version 1.1). Eur J Cancer 2009;45:228–47.
17. Weber LM, Nowicka M, Soneson C, Robinson MD. diffcyt: differential discovery in high-dimensional cytometry via high-resolution clustering. Commun Biol 2019;2:183.
18. Nowicka M, Krieg C, Crowell HL, Weber LM, Hartmann FJ, Guglietta S, et al. CyTOF workflow: differential discovery in high-throughput high-dimensional cytometry datasets. F1000Res 2017;6:748.
19. Abrecht C, Hallisey M, Dennis J, Nazzaro M, Brainard M, Hathaway E, et al. Simplified mass cytometry protocol for in-plate staining, barcoding, and cryopreservation of human PBMC samples in clinical trials. STAR Protoc 2022;3: 101362.
20. Lin JR, Izar B, Wang S, Yapp C, Mei S, Shah PM, et al. Highly multiplexed immunofluorescence imaging of human tissues and tumors using t-CyCIF and conventional optical microscopes. Elife 2018;7:e31657.
21. Schapiro D, Sokolov A, Yapp C, Chen YA, Muhlich JL, Hess J, et al. MCMICRO: a scalable, modular image-processing pipeline for multiplexed tissue imaging. Nat Methods 2022;19:311–5.
22. Iijima Y, Sakakibara R, Ishizuka M, Honda T, Shirai T, Okamoto T, et al. Notable response to nivolumab during the treatment of SMARCA4-deficient thoracic sarcoma: a case report. Immunotherapy 2020;12:563–9.
23. Florou V, Rosenberg AE, Wieder E, Komanduri KV, Kolonias D, Uduman M, et al. Angiosarcoma patients treated with immune checkpoint inhibitors: a case series of seven patients from a single institution. J Immunother Cancer 2019;7: 213.
24. Schöffski P, Ray-Coquard IL, Cioffi A, Bui NB, Bauer S, Hartmann JT, et al. Activity of eribulin mesylate in patients with soft-tissue sarcoma: a phase 2 study in four independent histological subtypes. Lancet Oncol 2011;12:1045–52.
25. Blay JY, Schöffski P, Bauer S, Krarup-Hansen A, Benson C, D'Adamo DR, et al. Eribulin versus dacarbazine in patients with leiomyosarcoma: subgroup analysis from a phase 3, open-label, randomised study. Br J Cancer 2019;120:1026–32.
26. Monga V, Skubitz KM, Maliske S, Mott SL, Dietz H, Hirbe AC, et al. A retrospective analysis of the efficacy of immunotherapy in metastatic soft-tissue sarcomas. Cancers 2020;12:1873.
27. Keung EZ, Burgess M, Salazar R, Parra ER, Rodrigues-Canales J, Bolejack V, et al. Correlative analyses of the SARC028 trial reveal an association between sarcoma-associated immune infiltrate and response to pembrolizumab. Clin Cancer Res 2020;26:1258–66.
28. Rosenbaum E, Antonescu CR, Smith S, Bradic M, Kashani D, Richards AL, et al. Clinical, genomic, and transcriptomic correlates of response to immune checkpoint blockade-based therapy in a cohort of patients with angiosarcoma treated at a single center. J Immunother Cancer 2022;10:e004149.
29. Walker JA, McKenzie ANJ. T(H)2 cell development and function. Nat Rev Immunol 2018;18:121–33.
30. Shi J, Song X, Traub B, Luxenhofer M, Kornmann M. Involvement of IL-4, IL-13 and their receptors in pancreatic cancer. Int J Mol Sci 2021;22:2998.
31. Wagner MJ, Othus M, Patel SP, Ryan C, Sangal A, Powers B, et al. Multicenter phase II trial (SWOG S1609, cohort 51) of ipilimumab and nivolumab in metastatic or unresectable angiosarcoma: a substudy of dual anti-CTLA-4 and anti-PD-1 blockade in rare tumors (DART). J Immunother Cancer 2021;9: e002990.
32. Gan Y, Li X, Han S, Liang Q, Ma X, Rong P, et al. The cGAS/STING pathway: a novel target for cancer therapy. Front Immunol 2021;12:795401.
33. Lebbe C, Garbe C, Stratigos AJ, Harwood C, Peris K, Marmol VD, et al. Diagnosis and treatment of Kaposi's sarcoma: European consensus-based interdisciplinary guideline (EDF/EADO/EORTC). Eur J Cancer 2019;114:117–27.
34. Bielack SS, Smeland S, Whelan JS, Marina N, Jovic G, Hook JM, et al. Methotrexate, doxorubicin, and cisplatin (MAP) plus maintenance pegylated interferon Alfa-2b versus MAP alone in patients with resectable high-grade osteosarcoma and good histologic response to preoperative MAP: first results of the EURAMOS-1 good response randomized controlled trial. J Clin Oncol 2015;33: 2279–87.
35. Keenan TE, Guerriero JL, Barroso-Sousa R, Li T, O'Meara T, Giobbie-Hurder A, et al. Molecular correlates of response to eribulin and pembrolizumab in

hormone receptor-positive metastatic breast cancer. Nat Commun 2021;12:5563.
36. Petitprez F, de Reyniès A, Keung EZ, Chen TW, Sun CM, Calderaro J, et al. B cells are associated with survival and immunotherapy response in sarcoma. Nature 2020;577:556–60.
37. Fridman WH, Meylan M, Petitprez F, Sun CM, Italiano A, Sautès-Fridman C. B cells and tertiary lymphoid structures as determinants of tumour immune contexture and clinical outcome. Nat Rev Clin Oncol 2022;19:441–57.
38. Vanhersecke L, Bougouin A, Crombé A, Brunet M, Sofeu C, Parrens M, et al. Standardized pathology screening of mature tertiary lymphoid structures in cancers. Lab Invest 2023;103:100063.
39. Gaglia G, Burger ML, Ritch CC, Rammos D, Dai Y, Crossland GE, et al. Lymphocyte networks are dynamic cellular communities in the immunoregulatory landscape of lung adenocarcinoma. Cancer Cell 2023;41:871–86.
40. Lin JR, Wang S, Coy S, Chen YA, Yapp C, Tyler M, et al. Multiplexed 3D atlas of state transitions and immune interaction in colorectal cancer. Cell 2023;186:363–81.
41. Plana D, Palmer AC, Sorger PK. Independent drug action in combination therapy: implications for precision oncology. Cancer Discov 2022;12:606–24.
42. Palmer AC, Izar B, Hwangbo H, Sorger PK. Predictable clinical benefits without evidence of synergy in trials of combination therapies with immune-checkpoint inhibitors. Clin Cancer Res 2022;28:368–77.
43. Palmer AC, Sorger PK. Combination cancer therapy can confer benefit via patient-to-patient variability without drug additivity or synergy. Cell 2017;171:1678–91.